

Metathesis Reactions of a Manganese Borylene Complex with Polar Heteroatom–Carbon Double Bonds: A Pathway to Previously Inaccessible Carbene Complexes

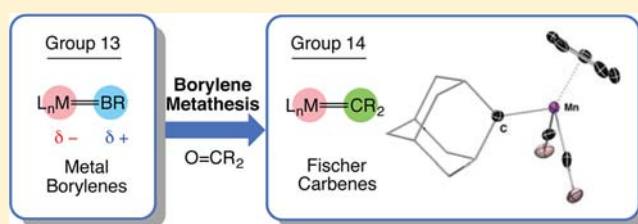
Jürgen Bauer, Holger Braunschweig,* Alexander Damme, Jose Oscar Carlos, Jimenez-Halla, Thomas Kramer, Krzysztof Radacki, Rong Shang, Eva Siedler, and Qing Ye

Institut für Anorganische Chemie, Julius-Maximilians-Universität Würzburg, Am Hubland, 97074 Würzburg, Germany

S Supporting Information

ABSTRACT: A comprehensive study has been carried out to investigate the metathesis reactivity of the terminal alkylborylene complex $[(\eta^5\text{-C}_5\text{H}_5)(\text{OC})_2\text{Mn}=\text{B}(\text{tBu})]$ (**1**). Its reactions with 3,3',5,5'-tetrakis(trifluoromethyl)benzophenone, 4,4'-dimethylbenzophenone, 2-adamantanone, 4,4'-bis(diethylamino)benzophenone, and 1,2-diphenylcyclopropen-3-one afforded the metathesis products $[(\eta^5\text{-C}_5\text{H}_5)(\text{OC})_2\text{Mn}=\text{CR}_2]$ ($\text{R} = \text{C}_6\text{H}_3\text{-3,5-(CF}_3)_2$ **3a**, $\text{C}_6\text{H}_4\text{-4-Me}$ **3b**, $\text{C}_6\text{H}_4\text{-4-NEt}_2$ **3d**; $\text{CR}_2 = \text{adamantylidene}$ **3c**, $\text{cyclo-C}_3\text{Ph}_2$ **3e**).

The cycloaddition intermediates were detected by NMR spectroscopy from reactions involving ketones with more electron-withdrawing substituents. The reaction of **1** with dicyclohexylcarbodiimide (DCC) only proceeds to form the cycloaddition product $[(\eta^5\text{-C}_5\text{H}_5)(\text{OC})_2\text{Mn}\{\kappa^2\text{-C}_6\text{H}_{10}\text{C(=N-Cy)N(Cy)B(tBu)}\}]$ (**4**), which upon warming, rearranges to afford complex $[(\eta^5\text{-C}_5\text{H}_5)(\text{OC})_2\text{Mn}\{\text{CN(Cy)B(tBu)CN(Cy)}\}]$ (**5**). The reaction of **1** with triphenylphosphine sulfide SPPH_3 also yields the metathesis product $[(\eta^5\text{-C}_5\text{H}_5)(\text{OC})_2\text{Mn}(\text{PPh}_3)]$ via an intermediate which is likely to be a η^2 -thioboryl complex $[(\eta^5\text{-C}_5\text{H}_5)(\text{OC})_2\text{Mn}\{\eta^2\text{-SB(tBu)}\}]$ (**6**). Similar reactions have been studied using an iron borylene complex $[(\text{Me}_3\text{P})(\text{OC})_3\text{Fe}=\text{B}(\text{Dur})]$ ($\text{Dur} = 2,3,5,6\text{-tetramethylphenyl}$, **9**). Extensive computational studies have been also carried out to gain mechanistic insights in these reactions, which provided reaction pathways that fit well with the experimental data.



INTRODUCTION

Since the discovery of complexes containing carbon–metal multiple bonds,¹ this area of chemistry has become one of the most important classes of compounds in organometallic chemistry for their role in many chemical processes, such as metathesis or polymerization of unsaturated organic substrates.^{2–4} Since the mid-1980s, the chemistry of metal–main group element unsaturated bond-containing systems that carry out metathesis reactions has also started to grow at an increasing rate, with the majority concerning group 4–6 transition metal–imide complexes which stoichiometrically or catalytically carry out imide/imine metatheses.^{5,6} Fewer examples of metal oxo^{6,7} and phosphinidene systems^{8,9} have also been reported (Figure 1).

Closely related to this class of compounds, borylene complexes that contain boron–metal double bonds, though being much younger,¹⁰ have demonstrated intriguing reactivity.^{11–15} Because the borylene ligand ($:\text{B}-\text{R}$) is isolobal to a carbene ligand and group 7 metal terminal borylene complexes such as $[(\eta^5\text{-C}_5\text{H}_5)(\text{OC})_2\text{Mn}=\text{B}(\text{tBu})]$ (**1**) are isoelectronic to group 6 metal carbyne complexes, it has been demonstrated that these complexes have reactivity that mirrors that of carbene and carbyne complexes,¹⁶ such as metathesis. Metal borylene complexes are unique among the previously reported metathesis systems in the respect that the metal center carries the

more negative charge relative to the boron center (Figure 2) and therefore may offer drastically different reactivities toward polar substrates from systems that polarize in the opposite direction.

This reactivity was first explored by Aldridge et al. employing a cationic group 8 iron terminal borylene complex $[(\eta^5\text{-C}_5\text{H}_5)(\text{OC})_2\text{Fe}=\text{BMes}]^+$, which showed reactivity toward Ph_3PS and Ph_3AsO , forming the metathesis products $[(\eta^5\text{-C}_5\text{H}_5)(\text{OC})_2\text{Fe}(\text{PPh}_3)]^+$ and $[(\eta^5\text{-C}_5\text{H}_5)(\text{OC})_2\text{Fe}(\text{AsPh}_3)]^+$ respectively.^{17,18} Later, we reported that the terminal group 7 metal borylene complexes $[\text{L}_n\text{M}=\text{BR}]$ underwent $[2 + 2]$ cycloaddition with unsaturated polar organic substrates (Scheme 1). In the case of **1** and benzophenone, the resulting cycloadduct is prone to subsequent cycloreversion to afford Fischer-type carbene complex $[(\eta^5\text{-C}_5\text{H}_5)(\text{OC})_2\text{Mn}=\text{CPh}_2]$ (**3**) via a cycloaddition intermediate $[(\eta^5\text{-C}_5\text{H}_5)(\text{OC})_2\text{Mn}\{\kappa^2\text{-B}_2\text{C}_2\text{B(tBu)OC(Ph}_2)\}]$ (**2**).¹⁹ This metathesis-type reactivity piqued our interest because it not only provided another clean and efficient way of preparing Fischer carbene complexes $[\text{L}_n\text{M}=\text{CR}_2]$ but also demonstrated a great potential of this class of complexes in stoichiometric or catalytic metathesis-type reactivity.

Received: April 5, 2013

Published: May 21, 2013

Group	3	4	5	6	7	8	9	13	14	15	16	17	18
										B	C	N	O	F	He
										Al	Si	P	S	Cl	Ne
....	Sc	Ti	V	Cr	Mn	Fe	Co	Ga	Ge	As	Se	Br	Kr	
....	Y	Zr	Nb	Mo	Tc	Ru	Rh	In	Sn	Sb	Te	I	Xe	
....	La	Hf	Ta	W	Re	Os	Ir	Tl	Pb	Bi	Po	At	Rn	
....	Ac	Rf	Db	Sg	Bh	Hs	Mt	Uut	Uuq	Uup	Uuh	Uus	Uuo	

Figure 1. Elements involved in transition metal–heteroatom metathesis systems.

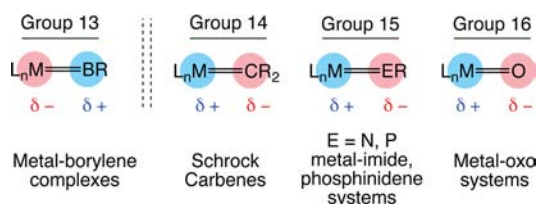
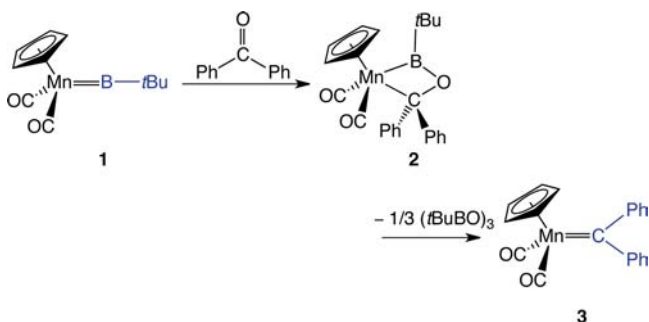


Figure 2. Systems containing unsaturated transition metal–main group element bonds that exhibit metathesis reactivity.

Scheme 1. Metathesis Reactions of the Terminal Borylene Complex **1** via the [2 + 2] Cycloaddition Intermediate **2**



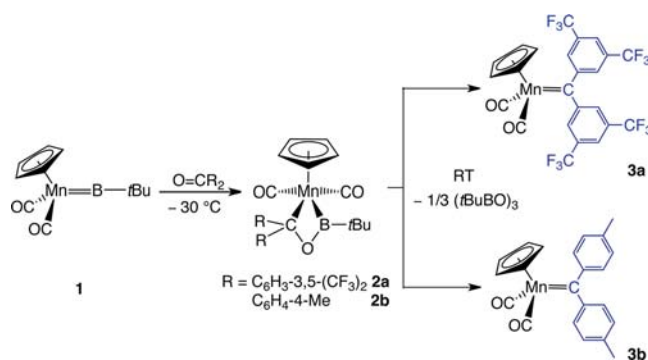
Complex **1** represents the first example of a group 7 metal–heteroatom complex that carries out metathesis, and this study examines such reactivity of **1** toward a range of substrates. The mechanistic pathways were probed computationally employing density functional theory (DFT) methods using the Gaussian03 series of programs (see Supporting Information for further details). A range of carbene complexes, including an unusual adamantylidene complex $[(\eta^5\text{-C}_5\text{H}_5)(\text{OC})_2\text{Mn}=\text{C}(\text{C}_9\text{H}_{14})]$ (**3c**), were synthesized and characterized. In addition, further exploration of the reaction of **1** and dicyclohexylcarbodiimide (DCC) led to discoveries of an unexpected rearrangement reaction. Furthermore, similar studies were extended to the neutral group 8 aryl-substituted iron borylene complex $[(\text{Me}_3\text{P})(\text{OC})_3\text{Fe}=\text{B}(\text{Dur})]$ (**9**, Dur = 2,3,5,6-tetramethylphenyl).

RESULTS AND DISCUSSION

Reactions with Ketones. In a fashion similar to that of the reaction of **1** with benzophenone,¹⁹ the reactions with 3,3',5,5'-tetrakis(trifluoromethyl)benzophenone and 4,4'-dimethylbenzophenone at -30°C in hexane lead to formation of [2 + 2] cycloaddition intermediates $[(\eta^5\text{-C}_5\text{H}_5)(\text{OC})_2\text{Mn}\{\kappa^2\text{-B,C-[B-(tBu)OCR}_2]\}]$ **2a** (R = $\text{C}_6\text{H}_3\text{-3,5-(CF}_3)_2$) and **2b** (R =

$\text{C}_6\text{H}_4\text{-4-Me}$), respectively. Upon being warmed to room temperature, the intermediates **2a** and **2b** were readily converted to carbene complexes **3a** and **3b** via cycloversion (Scheme 2). The conversion from **2a** to **3a** (24 h) took four times longer than that from **2b** to **3b** (6 h).

Scheme 2. Formation of **3a** and **3b** via the [2 + 2] Cycloaddition Intermediates **2a** and **2b**



The solution (hexane) IR spectrum of **2a** revealed two CO absorption bands at 2002 and 1928 cm^{-1} , considerably higher than those observed for the benzophenone adduct **2** (1988 and 1906 cm^{-1} , benzene).¹⁹ This is expected due to the more electron-withdrawing aryl substituents of **2a**. The ^{19}F NMR spectrum of **2a** shows two singlets at 63.0 and 63.3 ppm, corresponding to the six fluorine nuclei on each of the two aryl groups. Single crystals of **2a** were also obtained, and X-ray crystallographic studies were performed.²⁰ Selected bond lengths and angles are listed in Figure 3a. The bond distances of Mn–B1 (2.129(5) Å), B1–O3 (1.361(5) Å), and O3–C31 (1.465(5) Å) of **2a** are crystallographically identical to those observed for the analogous benzophenone adduct **2**. The Mn–B1 bond is significantly elongated compared to the starting borylene complex **1** (1.809(9) Å). The C31–Mn (2.153(1) Å) of **2a** is only marginally shorter than that observed for **2** (2.179(1) Å), which is counterintuitive considering the larger steric bulk of **2a**. The four-membered ring that composed of Mn–B1–O3–C31 is planar, with a sum of the internal angles of 359.6°.

The metathesis product **3a** gives rise to two carbonyl absorption bands at 2002 and 1944 cm^{-1} in hexane, unsurprisingly significantly higher than those of the benzophenone analogue **3** (1977 and 1919 cm^{-1}) due to the electron-withdrawing $[\text{CF}_3]$ groups of the aryl substituents.²¹ A singlet was observed at 332 ppm in the $^{13}\text{C}\{^1\text{H}\}$ NMR spectrum,

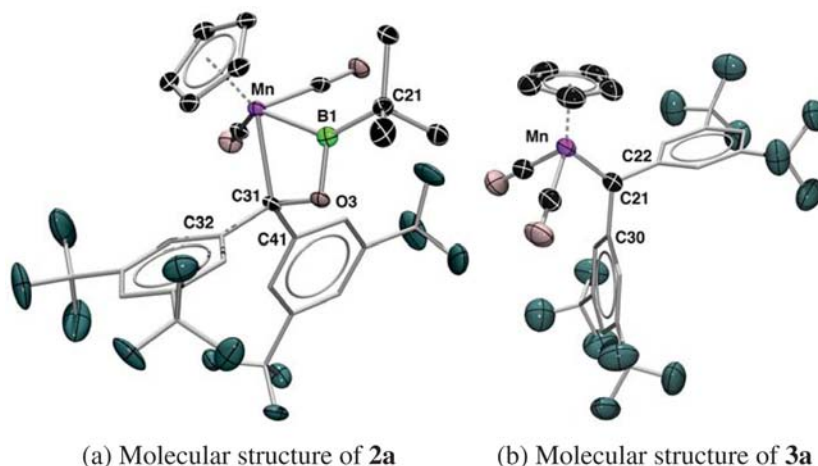
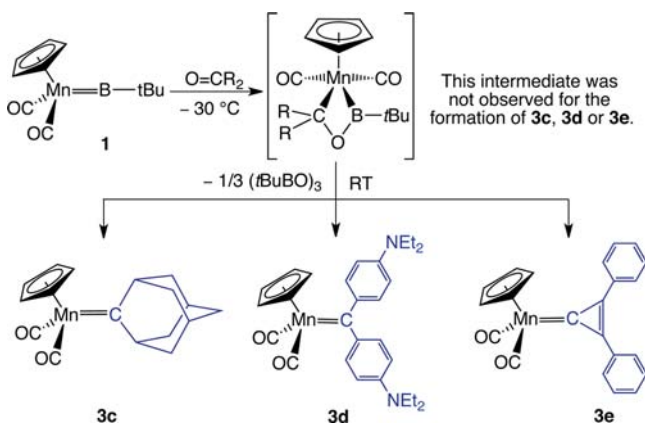


Figure 3. Molecular structures of **2a** and **3a** in the solid state. Thermal ellipsoids are shown at 50% probability. H atoms and the ellipsoids of the aryl rings have been omitted for clarity. Selected bond lengths (Å) and angles (deg) for **2a**: Mn–B1 2.129(5), Mn–C31 2.153(4), B1–O3 1.361(5), O3–C31 1.465(5), B1–C21 1.598(6); B1–Mn–C31 60.3(2), O3–B1–C21 117.7(4), O3–B1–Mn 102.5(3), B1–O3–C31 99.0(3), O3–C31–Mn 97.8(2); for **3a**: Mn1–C21 1.840(5), C30–C21–C22 109.8(4).

which was attributed to the carbene carbon nucleus. The ^{19}F NMR spectrum showed a singlet at 62.8 ppm, in the same region to those observed for **2a**.

The reactions of **1** with the more electron-releasing ketones, namely 2-adamantanone, 4,4'-bis(diethylamino)benzophenone, and 1,2-diphenylcyclopropen-3-one, proceeded to afford complexes $[(\eta^5\text{-C}_5\text{H}_5)(\text{OC})_2\text{Mn}=\text{CR}_2]$ (CR_2 = adamantylidene (**3c**), cyclo- $[\text{C}_3\text{Ph}_2]$ (**3e**), and $\text{R} = \text{C}_6\text{H}_5\text{-4-NEt}_2$ (**3d**)), respectively (Scheme 3) at a higher rate. The ^{11}B NMR spectra

Scheme 3. Formation of **3c**, **3d**, and **3e**^a



^aThe cycloaddition intermediates were not detected during the course of the reactions by NMR spectroscopy.

of the reaction mixtures obtained immediately after addition of the substrates showed signals of a mixture of the starting material **1** and the byproduct boroxine $[\text{B}(\text{tBuO})_3]$ at $-30\text{ }^\circ\text{C}$. In all cases, the reaction was complete within 1 h, more rapidly than those involving ketones with more electron-withdrawing substituents. Furthermore, no signal for the cycloaddition intermediate was detected during the course of these reactions.

Selected IR and NMR data of **3a–e** and related compounds from the literature are summarized in Table 1. The electronic effects of the carbene substituents are nicely reflected by the energies of the CO absorptions bands from solution IR spectroscopy. As expected, **3a** displayed the highest absorption bands at 2002 and 1944 cm^{-1} . Those observed for compounds **3b** and **3c** were similar, at 1977, 1915 and 1973, 1911 cm^{-1} respectively. Compound **3d** showed a pair of CO absorption bands at 1950, 1896 cm^{-1} , higher than those of **3a–c**, as expected. Those observed for compound **3e** are at 1948, 1886 cm^{-1} , very similar to those of **3d**.²² From this, a correlation between the electronic effects of the carbene substituents and the rate of metathesis reactions could be established. The more electron-releasing substrates (**3c** to **3e**) allowed more facile metathesis reactivity than those of electron-withdrawing (**3** to **3b**).

The NMR spectrum of compounds **3a–e** are largely unremarkable. The $^{13}\text{C}\{^1\text{H}\}$ NMR chemical shifts of the carbene carbon nuclei fall at the upper end of the typical range for carbene and alkylidene ligands, ranging between 332 and 398 ppm^{4,23} with the exception of the previously reported complex $[(\eta^5\text{-C}_5\text{H}_4\text{Me})(\text{OC})_2\text{Mn}=\text{C}\{\text{CPh}\}_2]$, at 234 ppm.²⁴

Table 1. Selected IR and NMR Data of Complexes $[(\eta^5\text{-C}_5\text{H}_5)(\text{OC})_2\text{Mn}=\text{CR}_2]$

compound	R	IR, ^a $\nu(\text{CO})$	NMR			
			δ_{C} (Mn=C)	δ_{C} (CO)	δ_{H} (Cp)	
3 ^{19,25}	Ph	1977, 1919	353	–	4.37	intermediate observed
3a	3,5- $\text{C}_6\text{H}_3(\text{CF}_3)_2$	2002, 1944	332	231	4.08	intermediate observed
3b	<i>p</i> -Tol	1977, 1915	353	233	4.43	intermediate observed
3c	adamantylidene	1973, 1911	389	233	4.45	no intermediate observed
3d	<i>p</i> - $\text{C}_6\text{H}_4(\text{NEt}_2)$	1950, 1896	344	234	4.61	no intermediate observed
3e	CPh	1948, 1886	234	233	4.70	no intermediate observed

^aMeasured in hexane.

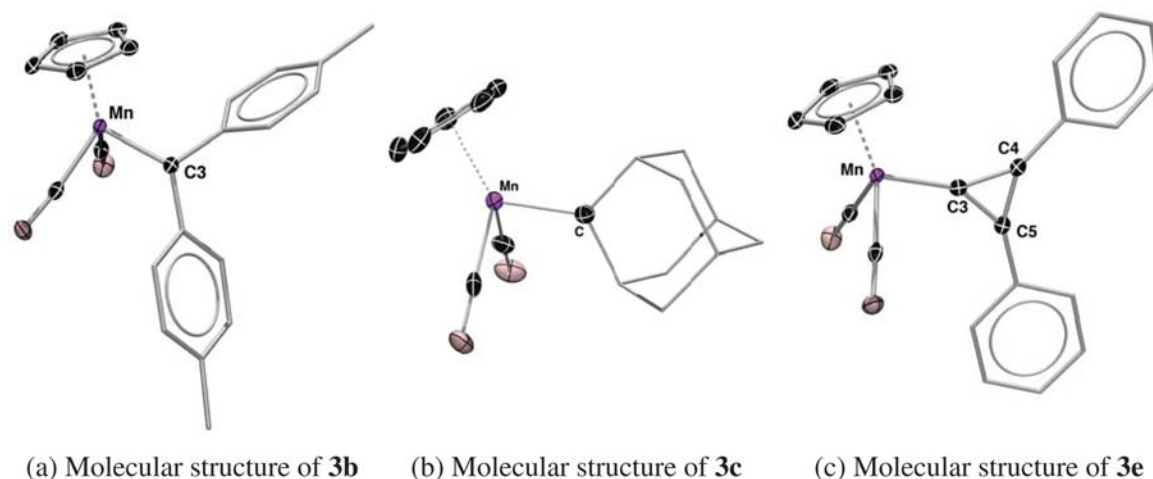


Figure 4. Molecular structures of **3b**, **3c**, and **3e** in the solid state. Thermal ellipsoids are shown at 50% probability. H atoms and the ellipsoids of the aryl and adamantylidene groups have been omitted for clarity. Selected bond lengths (Å) and angles (deg) for **3b**: Mn1–C3 1.877(2); for **3c**: Mn1–C11 1.862(4), C11–C16 1.526(5), C11–C12 1.528(5), C16–C11–C12 108.5(3); for **3e**: Mn–C3 1.899(1), C3–C5 1.412(2), C3–C4 1.420(2), C5–C4 1.344(2), C4–C3–C5 56.67(9).

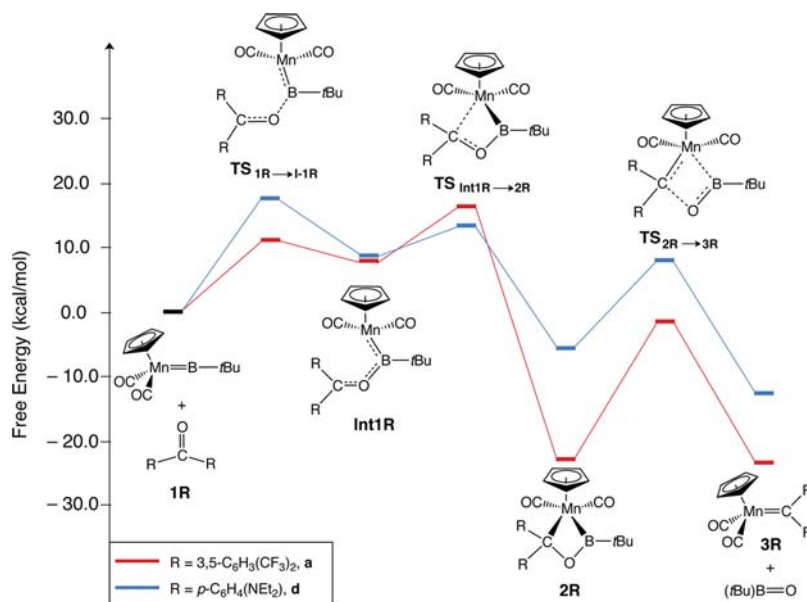


Figure 5. Proposed mechanism for the metathesis reactions of **1**.

The most deshielded carbene carbon nucleus of all was from the adamantylidene complex **3c**, close to 400 ppm, which is more deshielded than most carbyne and alkylidyne complexes.³

Complexes **3b**, **3c**, and **3e** were subjected to X-ray crystallographic studies (Figure 4). To the best of our knowledge, compound **3c** represents the first example of a structurally unsupported adamantylidene complex. Though a handful transition metal complexes with adamantyl ligands have been reported, all of them are structurally supported by other (often better) donor atoms coligated to the metal.^{26–32} The solid-state structure of **3c** showed a Mn=C bond length of 1.862(4) Å, which is significantly shorter than those observed for the adamantyl-ligated complexes (2.054–2.189 Å)^{26,27,31} but in the range typically observed for manganese carbene complexes (1.853–2.038 Å).^{24,25,33–41} The angle of C16–C11–C12 is 108.5(3)°, very close to that observed for the free adamantane molecule (109.60°).⁴² The structures of **3a** (Figure 3b), **3c** and **3e** (Figure 4) exhibit almost C_s symmetry where

the [:CR₂] unit lies approximately on the mirror plane bisecting the [(η⁵-C₅H₅)M(CO)₂] moiety. This has been reported for other Fischer carbene complexes;^{39,43} however, it contrasts with **3b**, where the [:CTol₂] plane cuts along one of the M–CO bonds.⁴⁴

We have performed DFT calculations at the PBE0/6-311+G(2d,p)//PBE0/(Cr:Wachters, 6-31G(2d,p)) level to gain a deeper understanding of the experimentally observed substituent effects. The formations of **3a–e** were computed separately, and the results showed a common mechanistic pathway (Figure 5). These overall exergonic processes start with the generation of the boryl complexes **Int1R** by the coordination of oxygen to the borylene ligand, which is an endergonic step. Subsequently, the carbenoid moiety coordinates to the manganese center, forming the intermediate **2R** via a transition state **TS_{Int1R→2R}**. The conversion of **2R** to the carbene complexes **3R** proceeds through another transition state, **TS_{2R→3R}**, which is analogous to what was proposed for

Table 2. Reaction Energies (ΔG_0^{298}) and Energy Barriers (ΔG^\ddagger) of the Proposed Reaction Mechanism for the Formation of 3 and 3a–e^a

		R = Ph	R = 3,5-C ₆ H ₃ (CF ₃) ₂ , a	R = <i>p</i> -Tol, b	R = adamantylidene, c	R = <i>p</i> -C ₆ H ₄ (NEt ₂), d	R = CPh, e
ΔG_0^{298}	1R → Int1	5.07	8.21	4.54	6.67	8.65	5.11
	Int1 → 2R	-21.41	-30.94	-19.94	-17.26	-14.25	-20.46
	2R → 3R	-2.68	-0.55	-2.44	-9.00	-7.01	-15.27
ΔG^\ddagger	TS _{1R→Int1R}	11.36	11.33	11.84	12.27	17.56	11.36
	TS _{Int1R→2R}	7.73	8.38	7.29	10.30	4.84	4.17
	TS _{2R→3R}	17.79	21.08	19.90	11.00	13.56	10.39

^aComputations were performed at PBE0/mixed-basis level. Values are given in kcal/mol.

Aldridge's reaction involving an isocyanate and $[(\eta^5\text{-C}_5\text{H}_5)\text{(OC)}_2\text{Fe}=\text{B}=\text{NCy}_2]^+$.⁴⁵

Figure 5 illustrates the overall mechanistic proposal for the metathesis reactions of 1R. The energies involved in the formation of 3a and 3d are mapped to demonstrate the electron-withdrawing and -donating effects of the substituents. An energy diagram including all the computational results for 3–3e is available in the Supporting Information, and all the reaction energies and energy barriers are summarized in Table 2. From the reaction energies (ΔG_0^{298}), it can be seen that the formation of 2R from Int1R is the most exergonic step in these reactions and is thermodynamically more favored in reactions involving more electron-withdrawing substituents (R = 3,5-C₆H₃(CF₃)₂: -30.94 and Ph: -21.41 kcal/mol). On the other hand, from the reaction barriers (ΔG^\ddagger), it can be seen that reactions involving more electron-withdrawing substituents require higher activation energy for the final cycloreversion step from 2R to 3R (R = 3,5-C₆H₃(CF₃)₂: 21.08, Ph: 17.79 and *p*-Tol: 19.90 kcal/mol) than those involving more electron-donating ones (CR₂ = adamantylidene: 11.00, R = *p*-C₆H₄(NEt₂): 13.56, and CPh: 10.39 kcal/mol). These together imply that the rate-determining step of this process varies depending on the substituents of the substrates. In the cases involving more electron-withdrawing substrates (R = 3,5-C₆H₃(CF₃)₂, Ph, and *p*-Tol), the cycloreversion step 2R → 3R is the rate-determining step with 2R residing in a deeper energy well. In other cases (CR₂ = adamantyl, R = *p*-C₆H₄(NEt₂), and CPh), the rate-determining step is the endergonic generation of Int1R, a point from which the reactions proceed until the formation of the metathesis products. This is in excellent agreement with the selectively observed cycloaddition intermediates 2, 2a, and 2b. The [OB(*t*Bu)] fragments further trimerize to form boroxine, which is a very exergonic reaction step and thus is presumed as the driving force of these reactions.

Reactions with Dicyclohexylcarbodiimide. Previously we reported the reaction of 1 and dicyclohexylcarbodiimide (DCC), which led to formation of the cycloaddition product $[(\eta^5\text{-C}_5\text{H}_5)(\text{OC})_2\text{Mn}\{\kappa^2\text{-C}_6\text{H}_{11}\text{C}(\text{=N}\text{C}_6\text{H}_{11})\text{N}(\text{C}_6\text{H}_{11})\text{B}(\text{C}_6\text{H}_{11})\}]$ 4.¹⁹ In attempt to force the further cycloreversion step, the reaction mixture was warmed to 65 °C. After several hours, 4 was converted to a new compound 5, which displayed a slightly broad ¹¹B signal at 47.0 ppm. One singlet at 310 ppm in the ¹³C{¹H} spectrum was assigned to the carbene carbon nucleus, which is significantly downfield-shifted compared to 4 (151 ppm), as expected for the increased bond order between manganese and carbon.

X-ray crystallographic studies revealed the structure of 5 to be $[(\eta^5\text{-C}_5\text{H}_5)(\text{OC})_2\text{Mn}=\text{C}\{\text{N}(\text{C}_6\text{H}_{11})\text{B}(\text{C}_6\text{H}_{11})\text{N}(\text{C}_6\text{H}_{11})\}]$ (Figure 6). The Mn–C1 distance of 1.894(2) Å is significantly shorter than that of its starting material 4 (2.056(4) Å),¹⁹ which is

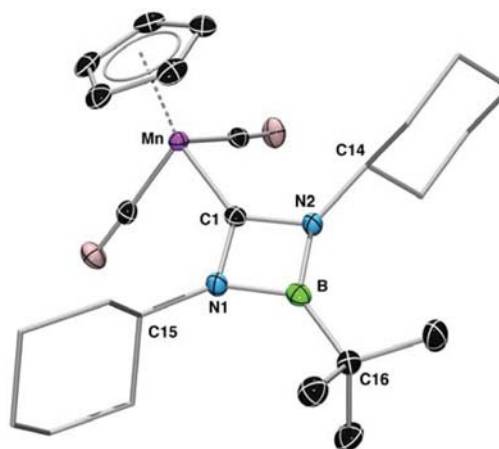


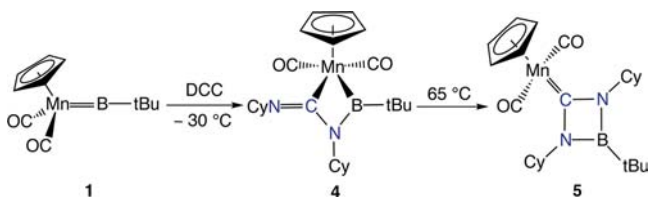
Figure 6. Structure of 5 in the solid state. Thermal ellipsoids are shown at 50% probability. H atoms and the ellipsoids of the cyclohexyl groups have been omitted for clarity. Selected bond lengths (Å) and angles (deg): Mn–C1 1.894(2), C1–N1 1.399(2), C1–N2 1.404(2), N1–B 1.474(3), N2–B 1.466(3), B–C16 1.573(3); N2–C1–N1 94.2(1), C1–N1–B 88.5(1), C1–N2–B 88.6(1), N1–B–N2 88.6(1).

expected for the increased bond order of Mn–C1. The bond distances of C1–N1 and C1–N2 are 1.399(2) and 1.404(2) Å, respectively, very similar to that observed for the (Mn)C–N(B) distance (1.413(5) Å) in complex 4. The four-membered ring C1–N1–B–N2 is planar, reflected by the sum of internal angles of 359.9°. The boron atom displays an expected planar geometry.

The insertion of carbodiimides into B=N bonds has been reported, and an initial [2 + 2] cycloaddition intermediate step was proposed in these reactions.⁴⁶ The formation of L_nM{=CN(Cy)B(R)N(Cy)} from metathesis-type reactivity has been reported by Aldridge et al. from the stoichiometric reaction of the cationic aminoborylene complex $[(\eta^5\text{-C}_5\text{H}_5)(\text{OC})_2\text{Fe}=\text{BNR}_2]^+[\text{BAR}_4^F]^-$ (R = Cy, *i*Pr, [BAR₄^F]⁻ = [B{C₆H₃-3,5-(CF₃)₂}]₄⁻), and dicyclohexylcarbodiimide (DCC) in dichloromethane. In this case, an intermediate akin to 5 has also been isolated. However, any presence of excess of DCC leads to formation of the double insertion product $[(\eta^5\text{-C}_5\text{H}_5)(\text{OC})_2\text{Fe}=\text{C}(\text{NCy})_2\text{B}(\text{NCy})_2\text{CNCy}_2]^+[\text{BAR}_4^F]^-$.⁴⁷ By comparison, our reaction proceeds much more slowly and thus allows the isolation of the cycloaddition product 4, which then rearranges to form the thermodynamically more stable complex 5 (Scheme 4).

We also carried out DFT calculations at PBE0/6-311+G-(2d,p)//PBE0/(Cr:Wachters, 6-31G (2d,p)) level to gain more mechanistic insight into this rearrangement. A overall mechanistic proposal is depicted in Figure 7. The reaction begins with a nucleophilic attack at the boron atom of 1 by a

Scheme 4. Formation of the [2 + 2] Cycloaddition Product $[(\eta^5\text{-C}_5\text{H}_5)(\text{OC})_2\text{Mn}\{\kappa^2\text{-C,B-C(=NCy)N(Cy)B(tBu)}\}]$ (4) and Its Rearrangement Reaction



nitrogen atom of DCC, which leads to formation of a boryl species **A1** via an activation barrier (**TS1**) of 13.6 kcal/mol. The intermediate **A1** then proceeds to form the observed product **4** by further coordination of the carbon (**TS2**) to the manganese center, which is an almost barrierless process (0.3 kcal/mol). Our calculations predict that the formation of **4** from **1** and DCC is an overall exergonic process (−8.7 kcal/mol) with a fairly shallow energy barrier (13.6 kcal/mol), which agrees well with the low temperature employed (−30 °C) for the isolation of **4**.

Instead of the coordination of the carbon atom to manganese via **TS2**, the second nitrogen atom of the **A1** may also attack the boron atom via an η^2 -coordinating **TS3** to form $\eta^1(\text{N})$ -coordinating intermediate **A2**,⁴⁸ which is a slightly exergonic process (−7.9 kcal/mol) at a reasonable cost of 7.9 kcal/mol. Subsequently, the carbene atom attacks the metal to reform an η^2 -bound transition state (**TS4**) (8.2 kcal/mol) before finally establishing the Mn–C double bond in **5**, which is the thermodynamic product of the reaction (−33.7 kcal/mol). This proposal suggests that the energy barrier required for formation of **5** from **4** is 26.4 kcal/mol, which implies a necessity for gentle heating. This is consistent with the experimental conditions employed for the rearrangement from **4** to **5**.

Jemmis, Aldridge, and co-workers also reported computational studies on the iron borylene reactions using $[(\eta^5\text{-C}_5\text{H}_5)(\text{OC})_2\text{Fe}=\text{B}=\text{NMe}_2]^+$ and carbodiimide (MeN=C=NMe) as models. Despite the structural similarities between their system and ours, a different mechanistic pathway was

proposed for the formation of the $[(\eta^5\text{-C}_5\text{H}_5)(\text{OC})_2\text{Fe}=\{\text{CN}(\text{R})\text{B}(\text{NMe}_2)\text{N}(\text{R})\}]^+$ (analogue of **5**) from an analogous intermediate $[(\eta^5\text{-C}_5\text{H}_5)(\text{OC})_2\text{Fe}=\text{B}(\text{NMe}_2)\text{N}(\text{R})(\text{CNR})]^+$ (**A1**), most likely due to the electronic differences between the amino and alkyl substituent of the boron. The extra π -stabilization from the amino group allows an Fe–B cleavage and subsequent rotation over the N–C–N–B dihedral angle to form the new N–B bond, completing the reaction.⁴⁵ This route has also been explored in our studies, and the results show that the Mn–B bond cleavage proceeds through a rather high transition state of ca. 35 kcal/mol. Furthermore, the C–N bond is also broken due to the strong polarity of the Cy–N–B–tBu fragment, thus prohibiting the subsequent rotation, which would lead to formation of **5**, and forming a isocyanide complex $[(\eta^5\text{-C}_5\text{H}_5)(\text{OC})_2\text{Mn}=\text{C}=\text{NCy}]$.

Reactions with the Triphenylphosphine Sulfide. Other polarized unsaturated substrates have also been investigated. Previously, Aldridge et al. had reported a successful reaction of $[(\eta^5\text{-C}_5\text{H}_5)(\text{OC})_2\text{FeB}(\text{NiPr}_2)]^+[\text{BAR}_4^F]^-$ with SPPH₃, from which the metathesis product $[(\eta^5\text{-C}_5\text{H}_5)(\text{OC})_2\text{Fe}(\text{PPh}_3)]^+[\text{BAR}_4^F]^-$ was isolated in excellent yield (>95%).¹⁸ A similar reaction was carried out with **1** and SPPH₃ in hexane at room temperature. An intermediate (**6**) was detected by NMR spectroscopy immediately after the addition of the SPPH₃, displaying a broad ¹¹B singlet at 88.6 ppm. At the same time, free triphenylphosphine was detected in the ³¹P{¹H} NMR spectrum as a slightly broadened singlet, which was further confirmed by both ¹H and ¹³C{¹H} NMR spectra. After 16 h at room temperature, **6** converted to the final cycloreversion products $[(\eta^5\text{-C}_5\text{H}_5)(\text{OC})_2\text{Mn}(\text{PPh}_3)]$ ⁴⁹ (**7**, ³¹P{¹H} NMR: 93.5 ppm) and a boron-containing species⁵⁰ (**8**, ¹¹B NMR: 71.7 ppm. Scheme 5).

Scheme 5. Reaction of 1 with SPPH₃

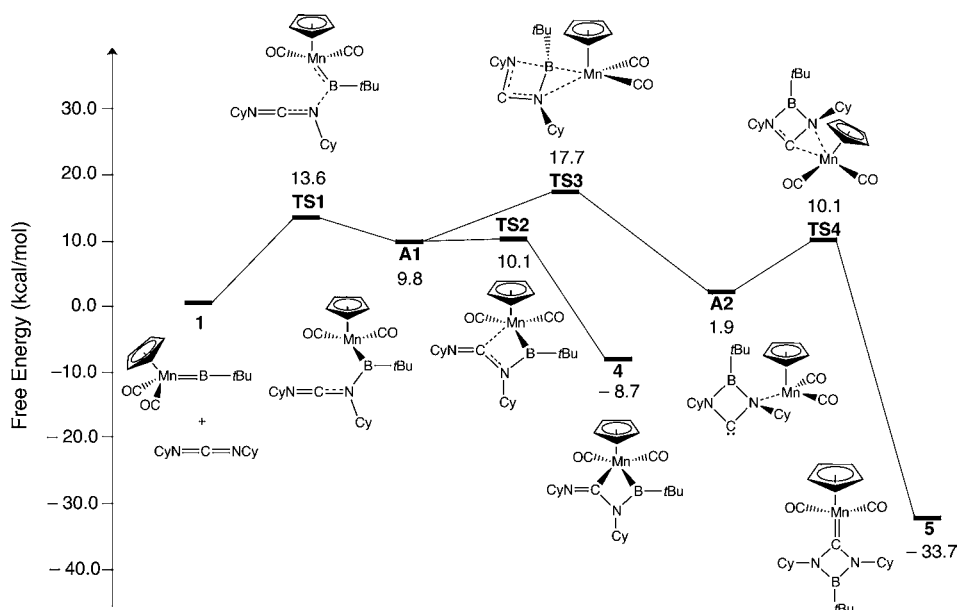
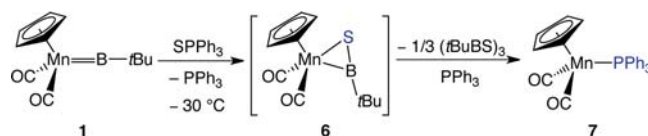


Figure 7. Proposed mechanism for formation of 4 and 5.

A mechanistic study employing PBE0/mixed-basis was carried out for the reaction of **1** and SPPH_3 to gain insight into the observed intermediate species **6**. The calculations showed that the formation of an intermediate either with a four-membered ring that was similar to **2R** (Figure 5), or that was isoelectronic to Aldridge's complex $[(\eta^5\text{-C}_5\text{H}_5)(\text{OC})_2\text{FeB}(\text{NiPr}_2)(\text{OPPh}_3)]^+[\text{BAR}_4^{\text{F}}]^-$ (or similar to **Int1R** in Figure 5),⁵¹ was not possible due to steric crowding as well as the polarization of the Mn–B–S–P fragment. [Calculations employing the same method and level of theory were also carried out for Aldridge's reaction involving $[(\eta^5\text{-C}_5\text{H}_5)(\text{OC})_2\text{FeBNiPr}_2]^+[\text{BAR}_4^{\text{F}}]^-$ and SPPH_3 as a reference.⁵¹ The results showed an intermediate that is consistent with the observed species, $[(\eta^5\text{-C}_5\text{H}_5)(\text{OC})_2\text{FeB}(\text{NiPr}_2)(\text{OPPh}_3)]^+$. The S–P bond persistently dissociated as the S–B bond formed to afford either **A1-S** and free triphenylphosphine, or a triphenylphosphine-coordinated species, **A2-S** (Figure 8),⁵²

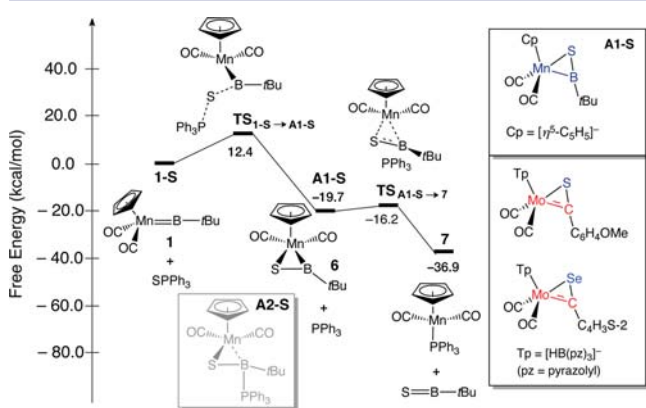


Figure 8. Proposed mechanism for the formation of **7**, featuring the proposed intermediate **6** (**A1-S** and **A2-S**) and Hill's thio- and selenoacyl analogues of **A1-S**.

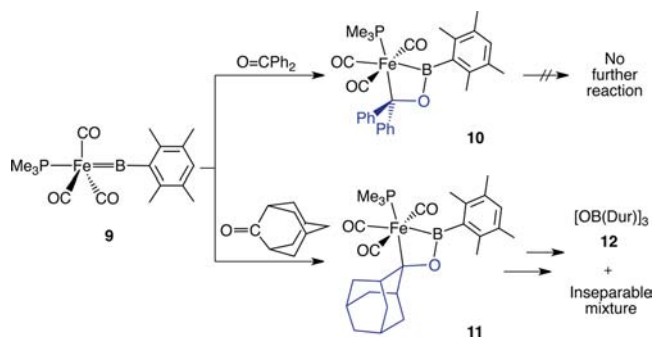
from which the free PPh_3 ligand subsequently exchanged with $[\text{S}=\text{B}(t\text{Bu})]$ to form the observed product **7**. Similar to reactions discussed previously, the $[\text{S}=\text{B}(t\text{Bu})]$ fragments oligomerize to form a cyclic species responsible for a singlet at 71.7 ppm in the ^{11}B NMR spectrum (**8**), which is likely to be the thermodynamic driving force of this reaction. [On the basis of earlier literature⁵⁰ and calculated ^{11}B chemical shift (67 ppm), the structure of **8** was proposed to be $[\text{SB}(t\text{Bu})]_3$. Unfortunately it could not be confirmed by either mass spectroscopy or X-ray crystallography.]

The calculated energy difference between **A1-S** and **A2-S** is a mere 3 kcal/mol, indicating **A2-S** being the energetically favored intermediate (−23.4 kcal/mol). However, the predicted ^{11}B NMR resonance of **A1-S** (86.3 ppm) matches the observed spectroscopic data of **6** (88.6 ppm) much better than that of **A2-S** (16.2 ppm). Also, free triphenylphosphine was observed in the reaction mixture by NMR spectroscopy. From these we presume **6** to be $[(\eta^5\text{-C}_5\text{H}_5)(\text{OC})_2\text{Mn}\{\eta^2\text{-SB}(t\text{Bu})\}]$ (**A1-S**, Scheme 5), which furthermore is isoelectronic to the well-studied chalcocacyl analogues (Figure 8).⁵³ This is drastically different to what was observed for the previously mentioned iron borylene system.^{18,54} In an attempt to isolate the observed intermediate **6**, reactions of **1** and S_8 (1 equiv of S atoms) in the absence of PPh_3 were performed. Although this reaction was much less selective, from which a complex mixture of products were obtained, complex **6** was identified from the NMR spectra, thus supporting our proposed structure **A1-S**.

The reactions of **1** with triphenylphosphine oxide OPPh_3 showed no reactivity even at elevated temperatures. Other substrates that have been explored for similar reactivities include PhNCS , PhNCO , and azo- and azido compounds. However, no controlled reactivity was observed.

Reactions of the Iron Borylene Complex $[(\text{Me}_3\text{P})(\text{OC})_3\text{Fe}=\text{B}(\text{Dur})]$. In attempt to extend this chemistry to other borylene systems, we performed similar experiments with our recently reported iron borylene complex $[(\text{Me}_3\text{P})(\text{OC})_3\text{Fe}=\text{B}(\text{Dur})]$ (**9**, Dur = 2,3,5,6-tetramethylphenyl).⁵⁵ The reaction of **9** with benzophenone leads to formation of the cycloaddition product $[(\text{Me}_3\text{P})(\text{OC})_3\text{Fe}\{\kappa^2\text{-B,C-[B}(\text{Dur})\text{OC}(\text{Ph})_2]\}]$ (**10**), from which the cycloreversion carbene product could not be isolated. With the results from the manganese system (Table 2), the reactions of **9** with 2-adamantanone and 1,2-diphenylcyclopropan-3-one were explored. In the presence of 2-adamantanone in hexane, the $[2 + 2]$ cycloaddition product **11** was isolated at low temperature (−30 °C), which upon warming to room temperature produced the boroxine $[\text{OB}(\text{Dur})]_3$ (**12**) as part of a mixture of products (Scheme 6).

Scheme 6. Reactions of Complex **9** with Ketones



The formation of the boroxine suggests that the intermediate **11** readily carries out the cycloreversion to produce the metathesis carbene complex, which may then subsequently decompose. The reaction involving 1,2-diphenylcyclopropan-3-one, on the other hand, showed no controlled reactivity. The ^{11}B NMR spectrum of the reaction mixture indicated formation of **12**.⁵⁶

X-ray crystallographic studies were carried out on crystals of **11**, and a picture of the solid-state molecular structure is shown in Figure 9. Complex **11** is isostructural to its analogue **10**. The Fe–B, Fe–C31, and C31–O bond distances are 2.101(3), 2.121(2), and 1.488(3) Å, respectively, slightly elongated compared to those observed for **10** (cf., 2.088(2), 2.112(1), and 1.469(2) Å), presumably due to the steric bulk of the adamantyl group. The ring composed of Fe–B–O–C31 is planar as was observed for **2a**, **2b**, **4**, **5**, and **10**.

CONCLUSION

A comprehensive study has been carried out to investigate the metathesis reactivity of borylene complex **1**. This complex reacts with a variety of different ketones to form a $[2 + 2]$ cycloaddition intermediate which undergoes a further cycloreversion step to yield a variety of Fischer-type manganese carbene species (**3a–e**), including the first adamantylidene complex (**3c**). The mechanisms and the substituent effect of the ketone substrates have also been studied employing PBE0/mixed-basis, which shows that ketones with more electron-releasing substituents form thermodynamically less stable

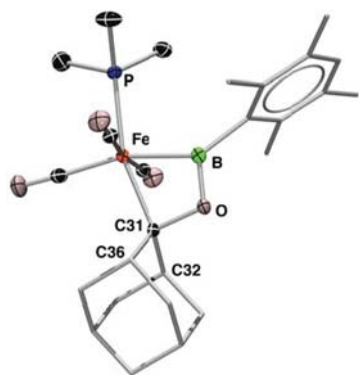


Figure 9. Structure of **11** in the solid state. Thermal ellipsoids are shown at 50% probability. H atoms and the ellipsoids of the cyclohexyl groups have been omitted for clarity. Selected bond lengths (Å) and angles (deg): Fe–B1 2.101(3), Fe–C31 2.121(2), Fe–P1 2.2339(7), B–O4 1.344(3), O–C31 1.488(3); B–Fe–P 100.37(8), C31–Fe–P 162.95(7), O–B–Fe 100.3(2), B–Fe–C31 62.7(1), B–O–C31 101.7(2), O–C31–Fe 94.7(1).

intermediates with smaller energy barriers to the cycloreversion carbene products compared to those with more electron-withdrawing substituents. This is consistent with the experimental observations.

The reaction of **1** with DCC produces an analogous cycloaddition product (**4**), which rearranges to form $[(\eta^5\text{-C}_5\text{H}_5)(\text{OC})_2\text{Mn}(\text{N}(\text{Cy})\text{B}(\text{tBu})\text{N}(\text{Cy}))]$ (**5**) at a slightly elevated temperature. Computational studies suggest a mechanistic pathway that involves an $\eta^1(\text{N})$ -coordinating carbene intermediate (**A2**). This is quite different to what has been reported previously for the reaction of $[(\eta^5\text{-C}_5\text{H}_5)(\text{OC})_2\text{Fe}=\text{B}=\text{NMe}_2]^+$ with a carbodiimide, from which the intermediate $[(\eta^5\text{-C}_5\text{H}_5)(\text{OC})_2\text{Fe}(\text{N}(\text{R})\text{B}(\text{NMe}_2))\{\text{N}(\text{R})\}]^+$ was proposed.⁴⁵

The reaction of **1** with SPPPh₃ also yielded the expected metathesis product (**7**). An intermediate was observed at low temperature. DFT calculations suggest a η^2 -thioboryl complex **6**, which is consistent with the experimentally obtained spectroscopic data.

Efforts have been put into extending this metathesis reactivity to other borylene systems. The iron arylborylene complex **9** exhibits such reactivity. A [2 + 2] cycloaddition product **11** has been isolated from its reaction with 2-adamantanone, which represents a rare example of an adamantyl–transition metal complex. Although spectroscopic evidence suggests that the cycloreversion reaction proceeds, the expected carbene product could not be isolated. Complex **1** remains the only borylene complex that reliably exhibits this metathesis reactivity.

■ ASSOCIATED CONTENT

📄 Supporting Information

The experimental section, X-ray crystallographic data, and details of computational studies are in the Supporting Information. This material is available free of charge via the Internet at <http://pubs.acs.org/>.

■ AUTHOR INFORMATION

Corresponding Author

h.braunschweig@mail.uni-wuerzburg.de

Notes

The authors declare no competing financial interest.

■ ACKNOWLEDGMENTS

We thank European Research Council (Advanced Investigator Grant to H.B.) for financial support.

■ REFERENCES

- (1) (a) Fischer, E. O.; Maasboel, A. *Angew. Chem.* **1964**, *76*, 645. (b) Fischer, E. O.; Kreis, G.; Kreiter, C. G.; Mueller, J.; Huttner, G.; Lorenz, H. *Angew. Chem.* **1973**, *85*, 618–20. (c) Fischer, E. O. *Adv. Organomet. Chem.* **1976**, *14*, 1–32.
- (2) (a) Wu, X.; Tamm, M. *Beilstein J. Org. Chem.* **2011**, *7*, 82–93. (b) Schrock, R. R.; Czekelius, C. *Adv. Synth. Catal.* **2007**, *349*, 55–77. (c) Bruce, M. I.; Low, P. J. *Adv. Organomet. Chem.* **2004**, *50*, 179–444. (d) Blackwell, J. M.; Figueroa, J. S.; Stephens, F. H.; Cummins, C. C. *Organometallics* **2003**, *22*, 3351–3353. (e) Choukroun, R.; Lorber, C.; Lepetit, C.; Donnadieu, B. *Organometallics* **2003**, *22*, 1995–1997. (f) Trnka, T. M.; Grubbs, R. H. *Acc. Chem. Res.* **2001**, *34*, 18–29. (g) McGrath, T. D.; Stone, F. G. A. *Adv. Organomet. Chem.* **2005**, *53*, 1–40. (h) Brothers, P. J. *Adv. Organomet. Chem.* **2000**, *46*, 223–321. (i) Brew, S. A.; Stone, F. G. A. *Adv. Organomet. Chem.* **1993**, *35*, 135–86. (j) Mayr, A.; Hoffmeister, H. *Adv. Organomet. Chem.* **1991**, *32*, 227–324. (k) Stone, F. G. A. *Adv. Organomet. Chem.* **1990**, *31*, 53–89. (l) Buhro, W. E.; Chisholm, M. H. *Adv. Organomet. Chem.* **1987**, *27*, 311–69. (m) Kim, H. P.; Angelici, R. J. *Adv. Organomet. Chem.* **1987**, *27*, 51–111. (n) Schrock, R. R. *Acc. Chem. Res.* **1986**, *19*, 342–348. (o) Turner, H. W.; Fellmann, J. D.; Rocklage, S. M.; Schrock, R. R.; Churchill, M. R.; Wasserman, H. J. *J. Am. Chem. Soc.* **1980**, *102*, 7809–11. (p) Rocklage, S. M.; Schrock, R. R. *J. Am. Chem. Soc.* **1982**, *104*, 3077–81.
- (3) Caldwell, L. M. *Adv. Organomet. Chem.* **2008**, *56*, 1–94.
- (4) Gallop, M. A.; Roper, W. R. *Adv. Organomet. Chem.* **1986**, *25*, 121–198.
- (5) (a) Bolton, P. D.; Mountford, P. *Adv. Synth. Catal.* **2005**, *347*, 355–366. (b) Hazari, N.; Mountford, P. *Acc. Chem. Res.* **2005**, *38*, 839–849. (c) Mayer, J. M. *Acc. Chem. Res.* **1998**, *31*, 441–450. (d) Wigley, D. E. *Prog. Inorg. Chem.* **1994**, *42*, 239–482. (e) Mountford, P. *Chem. Commun.* **1997**, 2127–2134. (f) Blake, A. J.; Collier, P. E.; Dunn, S. C.; Li, W.-S.; Mountford, P.; Shishkin, O. V. *J. Chem. Soc., Dalton Trans.* **1997**, 1549–1558.
- (6) Woo, L. K. *Chem. Rev.* **1993**, *93*, 1125–36.
- (7) (a) Birdwhistell, K. R.; Boucher, T.; Ensminger, M.; Harris, S.; Johnson, M.; Toporek, S. *Organometallics* **1993**, *12*, 1023–5. (b) Jolly, M.; Mitchell, J. P.; Gibson, V. C. *J. Chem. Soc., Dalton Trans.* **1992**, 1329–30. (c) Green, M. L. H.; Hogarth, G.; Konidaris, P. C.; Mountford, P. *J. Organomet. Chem.* **1990**, *394*, C9–15.
- (8) Shah, S.; Protasiewicz, J. D. *Coord. Chem. Rev.* **2000**, *210*, 181–201.
- (9) Dillon, K. B.; Gibson, V. C.; Sequeira, L. J. *J. Chem. Soc., Chem. Commun.* **1995**, 2429–30.
- (10) Braunschweig, H.; Wagner, T. *Angew. Chem., Int. Ed. Engl.* **1995**, *34*, 825–6.
- (11) Aldridge, S.; Coombs, D. L. *Coord. Chem. Rev.* **2004**, *248*, 535–559.
- (12) Anderson, C. E.; Braunschweig, H.; Dewhurst, R. D. *Organometallics* **2008**, *27*, 6381–6389.
- (13) Braunschweig, H.; Kollann, C.; Seeler, F. *Struct. Bonding (Berlin)* **2008**, *130*, 1–27.
- (14) Braunschweig, H.; Dewhurst, R. D.; Schneider, A. *Chem. Rev.* **2010**, *110*, 3924–3957.
- (15) Schmid, G.; Meyer-Zaika, W.; Boese, R.; Augart, N. *Angew. Chem., Int. Ed.* **1988**, *27*, 952–953.
- (16) Braunschweig, H.; Radacki, K.; Shang, R.; Tate, C. W. *Angew. Chem., Int. Ed.* **2013**, *52*, 729–733.
- (17) Coombs, D. L.; Aldridge, S.; Rossin, A.; Jones, C.; Willock, D. J. *Organometallics* **2004**, *23*, 2911–2926.
- (18) Kays, D. L.; Day, J. K.; Ooi, L.-L.; Aldridge, S. *Angew. Chem., Int. Ed.* **2005**, *44*, 7457–7460.
- (19) Braunschweig, H.; Buzler, M.; Radacki, K.; Seeler, F. *Angew. Chem., Int. Ed.* **2007**, *46*, 8071–8073.

(20) Details for X-ray crystallographic studies of all the structures are listed in Supporting Information. The structures were solved using direct methods, refined with the Shelx software package and expanded using Fourier techniques. Sheldrick, G. M. *Acta Crystallogr., Sect. A: Found. Crystallogr.* **2008**, *A64*, 112–122.

(21) Herrmann, W. A. *Chem. Ber.* **1975**, *108*, 486–99.

(22) The CO absorption bands from solution IR spectroscopy of **3d** are at 1950 and 1896 cm^{-1} , higher in energy than those of the reported complex $[(\eta^5\text{-C}_5\text{H}_4\text{Me})(\text{OC})_2\text{Mn}=\text{C}\{\text{CPh}\}_2]$ as expected (1935 and 1867 cm^{-1} , toluene). Kirchgaessner, U.; Schubert, U. *Organometallics* **1988**, *7*, 784. Kirchgaessner, U.; Piana, H.; Schubert, U. *J. Am. Chem. Soc.* **1991**, *113*, 2228–2232. Ofele, K.; Tosh, E.; Taubmann, C.; Herrmann, W. A. *Chem. Rev.* **2009**, *109*, 3408–3444. Scherer, W.; Tafipolsky, M.; Ofele, K. *Inorg. Chim. Acta* **2008**, *361*, 513–520.

(23) Brothers, P. J.; Roper, W. R. *Chem. Rev.* **1988**, *88*, 1293–326.

(24) (a) Kirchgaessner, U.; Schubert, U. *Organometallics* **1988**, *7*, 784. (b) Kirchgaessner, U.; Piana, H.; Schubert, U. *J. Am. Chem. Soc.* **1991**, *113*, 2228–32.

(25) Herrmann, W. A.; Hubbard, J. L.; Bernal, I.; Korp, J. D.; Haymore, B. L.; Hillhouse, G. L. *Inorg. Chem.* **1984**, *23*, 2978–83.

(26) Millard, M. D.; Moore, C. E.; Rheingold, A. L.; Figueroa, J. S. *J. Am. Chem. Soc.* **2010**, *132*, 8921–8923.

(27) Gerber, R.; Blacque, O.; Frech, C. M. *ChemCatChem* **2009**, *1*, 393–400.

(28) Diekmann, M.; Bockstiegel, G.; Luetzen, A.; Friedemann, M.; Saak, W.; Haase, D.; Beckhaus, R. *Organometallics* **2006**, *25*, 339–348.

(29) Bravo-Zhivotovskii, D.; Peleg-Vasserman, H.; Kosa, M.; Molev, G.; Botoshanskii, M.; Apeloig, Y. *Angew. Chem., Int. Ed.* **2004**, *43*, 745–748.

(30) Windhager, J.; Goerls, H.; Petzold, H.; Mloston, G.; Linti, G.; Weigand, W. *Eur. J. Inorg. Chem.* **2007**, 4462–4471.

(31) Endo, K.; Grubbs, R. H. *J. Am. Chem. Soc.* **2011**, *133*, 8525–8527.

(32) Keitz, B. K.; Endo, K.; Patel, P. R.; Herbert, M. B.; Grubbs, R. H. *J. Am. Chem. Soc.* **2012**, *134*, 693–699.

(33) Herrmann, W. A.; Weidenhammer, K.; Ziegler, M. L. *Z. Anorg. Allg. Chem.* **1980**, *460*, 200–6.

(34) Herrmann, W. A.; Plank, J.; Hubbard, J. L.; Kriechbaum, G. W.; Kalcher, W.; Koumbouris, B.; Ihl, G.; Schaefer, A.; Ziegler, M. L. *Z. Naturforsch., B: Anorg. Chem., Org. Chem.* **1983**, *38B*, 1392–8.

(35) Herrmann, W. A.; Plank, J.; Kriechbaum, G. W.; Ziegler, M. L.; Pfisterer, H.; Atwood, J. L.; Rogers, R. D. *J. Organomet. Chem.* **1984**, *264*, 327–52.

(36) DeShong, P.; Sidler, D. R.; Rybczynski, P. J.; Slough, G. A.; Rheingold, A. L. *J. Am. Chem. Soc.* **1988**, *110*, 2575–85.

(37) Friedrich, P.; Besl, G.; Fischer, E. O.; Huttner, G. *J. Organomet. Chem.* **1977**, *139*, C68–C72.

(38) Ortin, Y.; Coppel, Y.; Lugan, N.; Mathieu, R.; McGlinchey, M. J. *Chem. Commun.* **2001**, 1690–1691.

(39) Ortin, Y.; Lugan, N.; Mathieu, R. *Dalton Trans.* **2005**, 1620–1636.

(40) Tang, Y.; Sun, J.; Chen, J. *Organometallics* **1999**, *18*, 2459–2465.

(41) Sun, S.; Edwards, J. O.; Sweigart, D. A.; D'Accolti, L.; Curci, R. *Organometallics* **1995**, *14*, 1545–7.

(42) Amoureux, J. P.; Foulon, M. *Acta Crystallogr., Sect. B: Struct. Sci.* **1987**, *B43*, 470–9.

(43) Schilling, B. E. R.; Hoffmann, R.; Lichtenberger, D. L. *J. Am. Chem. Soc.* **1979**, *101*, 585–91.

(44) (a) Schilling, B. E. R.; Hoffmann, R.; Faller, J. W. *J. Am. Chem. Soc.* **1979**, *101*, 592–8. (b) Kostic, N. M.; Fenske, R. F. *J. Am. Chem. Soc.* **1982**, *104*, 3879–84. (c) Caulton, K. G. *Coord. Chem. Rev.* **1981**, *38*, 1–43.

(45) De, S.; Pierce, G. A.; Vidovic, D.; Kays, D. L.; Coombs, N. D.; Jemmis, E. D.; Aldridge, S. *Organometallics* **2009**, *28*, 2961–2975.

(46) (a) Jefferson, R.; Lappert, M. F.; Prokai, B.; Tilley, B. P. *J. Chem. Soc. A* **1966**, 1584–90. (b) Brauer, D. J.; Buchheim-Spiegel, S.; Buerger, H.; Gielen, R.; Pawelke, G.; Rothe, J. *Organometallics* **1997**, *16*, 5321–5330.

(47) (a) Pierce, G. A.; Aldridge, S.; Jones, C.; Gans-Eichler, T.; Stasch, A.; Coombs, N. D.; Willock, D. J. *Angew. Chem., Int. Ed.* **2007**, *46*, 2043–2046. (b) Pierce, G. A.; Coombs, N. D.; Willock, D. J.; Day, J. K.; Stasch, A.; Aldridge, S. *Dalton Trans.* **2007**, 4405–4412.

(48) Ishida, Y.; Donnadiou, B.; Bertrand, G. *Proc. Natl. Acad. Sci. U.S.A.* **2006**, *103*, 13585–13588.

(49) Ginzburg, A. G.; Fedorov, L. A.; Petrovskii, P. V.; Fedin, E. I.; Setkina, V. N.; Kursanov, D. N. *J. Organomet. Chem.* **1974**, *73*, 77–84.

(50) (a) Wiberg, E.; Sturm, W. *Angew. Chem.* **1955**, *67*, 483–93.

(b) Wiberg, E.; Sturm, W. *Z. Naturforsch.* **1955**, *10b*, 112–13.

(c) Siebert, W. *The chemistry of inorganic homo- and heterocycles*; Academic Press: New York, 1987; Vol. 1.

(51) Kays, D. L.; Rossin, A.; Day, J. K.; Ooi, L.-L.; Aldridge, S. *Dalton Trans.* **2006**, 399–410.

(52) Kreissl, F. R.; Ullrich, N.; Wirsing, A.; Thewalt, U. *Organometallics* **1991**, *10*, 3275–7.

(53) (a) Clark, G. R.; Marsden, K.; Roper, W. R.; Wright, L. J. *J. Am. Chem. Soc.* **1980**, *102*, 6570–1. (b) Gill, D. S.; Green, M.; Marsden, K.; Moore, L.; Orpen, A. G.; Stone, F. G. A.; Williams, I. D.; Woodward, P. *J. Chem. Soc., Dalton Trans.* **1984**, 1343–7. (c) Cook, D. J.; Hill, A. F. *Organometallics* **2003**, *22*, 3502–3512. (d) Caldwell, L. M.; Hill, A. F.; Willis, A. C. *Chem. Commun.* **2005**, 2615–2617.

(54) Kays, D. L.; Day, J. K.; Aldridge, S.; Harrington, R. W.; Clegg, W. *Angew. Chem., Int. Ed.* **2006**, *45*, 3513–3516.

(55) Braunschweig, H.; Ye, Q.; Radacki, K. *Chem. Commun.* **2012**, *48*, 2701–2703.

(56) ^{11}B NMR (C_6D_6 , 128.3 MHz) δ_{B} 33.3 ppm; ^1H NMR (C_6D_6 , 400.1 MHz): δ_{H} 2.11 (6 H), 2.37 (6 H), 6.95 (1H).